Approved for public release; distribution is unlimited.

Vehicle Signal Enhancement Using Packet Wavelet Transform and Nonlinear Noise Processing Techniques

Jose E. Lopez, Juei Cheng Lo, Jennifer Saulnier
CYTEL Systems, Inc.
Hudson, MA 01749

ABSTRACT

The role of signal preprocessors, such as normalization preprocessor, channel effects inversion preprocessor, de-noising preprocessor have become an important part of many vehicle identification systems in order to extend their utility and provide continued performance in the face of reduced SNR. This paper examines the role of developing a non-parametric vehicle signal enhancement preprocessor by employing packet wavelet transform (PWT) decomposition, nonlinear noise processing methods, and signal restoration via the inverse PWT signal reconstruction. This effort is part of a larger project aimed at developing an Integrated Vehicle Classification System Using Wavelet / Neural Network Processing of Acoustic/Seismic Emissions on a Windows PC performed under a Phase II SBIR for the US Army TACOM/ARDEC. This paper presents a systematized study of the application of PWT de-noising methods to acoustic combat vehicle signals. Using an acoustic combat vehicle signal segment, a linear model in the form of an ARMA filter is developed which closely mimics the dynamics of the vehicle time-series. This deterministic baseline model is mixed with scaled white noise to produce noise-corrupted signals of various SNRs. The PWT sensitivities examined include basis function families, (Daubechies, Coiflet, Symlets, Beylkin, Biorthogonal), basis function support and Packet Tree decomposition length. Nonlinear noise processing sensitivities examined include the major thresholding methods (Universal, Stein's Unbiased Risk Estimate (SURE), Minimax and Hybrid) and threshold application (Hard or Soft thresholding). Sensitivity analysis of these methods to the acoustic vehicle signal enhancement are presented along with a discussion concerning the reduction of this scheme to a preprocessor for a real-time vehicle monitor.

1. INTRODUCTION

This paper discusses the development and subsequent initial investigations for a vehicle signal preconditioning method based on the development of a set of wavelet-based, vehicle signal de-noising algorithms. The focus of this work has centered on the use of the multiresolution decomposition and reconstruction capabilities of the Packet Wavelet Transform (PWT) along with nonlinear processing methods for noise removal. The primary motivation is to ultimately determine the utility of applying real-time signal de-noising preprocessing to help in preconditioning of signals prior to classification for lower SNR situations and possibly for multi-vehicle scenarios. An attractive side-benefit to this effort is the future possibility of using the PWT directly as another set of vehicle feature extraction methods that can be used by a classifier for vehicle identification.

Our initial goals entailed developing a suite of software, which allow selecting various Packet Wavelet decomposition strategies, allow selection of a rich range of basis functions, and allow testing of various thresholds and their implementation schemes. This software suite will be initially integrated into the CYTEL Systems, Inc., "Vehicle Signal Analysis Environment (VSAE)" where it can be tested and analyzed on vehicle signal data. The following sections provide the pertinent theoretical underpinnings for using these techniques. It describes: 1) the set of basis functions implemented, 2) decompositions levels allowed, 3) details on the nonlinear noise processing strategies and 4) their implementation under the VSAE.

2. UNDERSTANDING THE PACKET WAVELET TRANSFORM (PWT)

2.1. WAVELETS AND FILTER BANKS

Conceptually, according to [2], a signal $s(t)$ can be expanded on an orthonormal basis for $L_2(R)$

Form SF298 Citation Data

Report Date *("DD MON YYYY")* 00001999	**Report Type** N/A	**Dates Covered (from... to)** *("DD MON YYYY")*

Title and Subtitle Vehicle Signal Enhancement Using Packet Wavelet Transform and Nonlinear Noise Processing Techniques	**Contract or Grant Number**
	Program Element Number
Authors	**Project Number**
	Task Number
	Work Unit Number
Performing Organization Name(s) and Address(es) CYTEL Systems, Inc. Hudson, MA 01749	**Performing Organization Number(s)**
Sponsoring/Monitoring Agency Name(s) and Address(es)	**Monitoring Agency Acronym**
	Monitoring Agency Report Number(s)
Distribution/Availability Statement Approved for public release, distribution unlimited	
Supplementary Notes	
Abstract	
Subject Terms	
Document Classification unclassified	**Classification of SF298** unclassified
Classification of Abstract unclassified	**Limitation of Abstract** unlimited
Number of Pages 27	

$$s(t) = \sum_{k} c_{j0}(k)\phi_{j0,k}(t) + \sum_{k}\sum_{j=j0}^{\infty} d_j(k)\psi_{j,k}(t) \tag{2.1}$$

where $\psi_{j,k}(t)$ are the wavelet functions and $\phi_{j0,k}(t)$ are the scaling functions. The wavelet functions are derived from a single "mother-wavelet" through dilations and translations. Analysis digital filter banks (DFB) are used to implement the expansion to scaling and wavelet functions in discrete time. There is another DFB called the synthesis DFB. It is used to reconstruct the input signal from the decomposed wavelet coefficients.

The link between the DFB and continuous time wavelets is in the limit of a logarithmic filter tree:

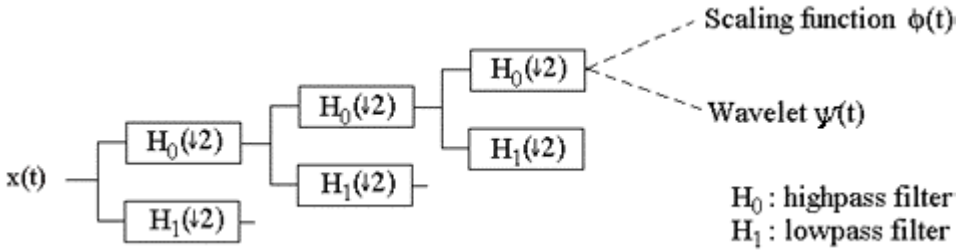

Figure 2.1 Scaling Function and Wavelets from Iteration of the Lowpass Filter [3].

The Packet Wavelet Transform (PWT), however, is a full tree version of the discrete wavelets. An analysis DFB to generate packet wavelets is shown in Figure 2.2.

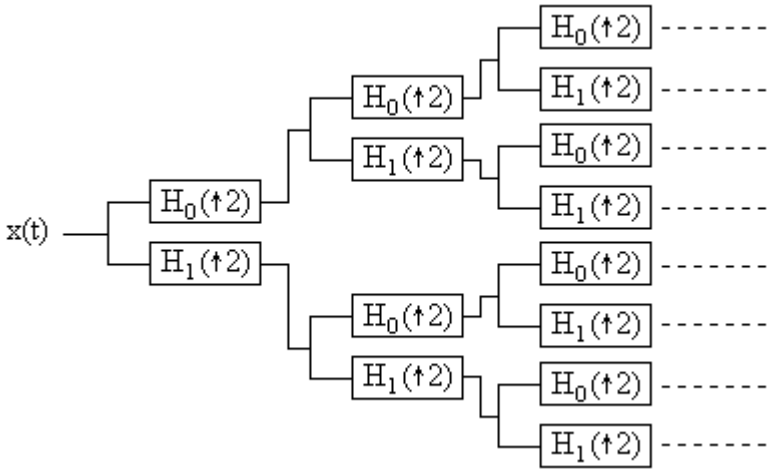

Figure 2.2 A full Tree Digital Filter Bank (DFB)

2.2. DECOMPOSITION AND RECONSTRUCTION

To simplify the idea, a two-channel DFB (analysis and synthesis) is used to explain the process of decomposition and reconstruction.

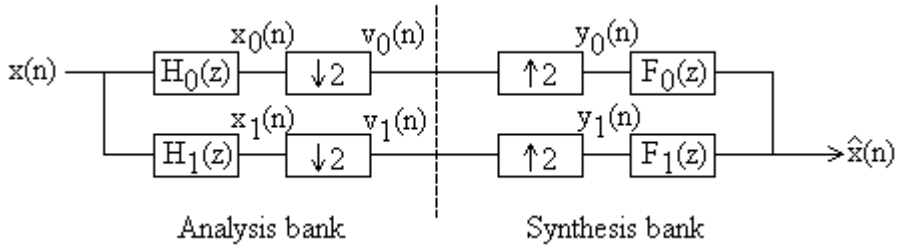

Figure 2.3 Analysis and Synthesis Filter Bank

The analysis DFB is constructed from stages comprising two downsamplers and two filters (one highpass and the other lowpass,) and the synthesis DFB comprises two upsamplers and two filters. In practice, the analysis filters have nonzero transition bandwidth and stopband gain. The signals $x_0(n)$ and $x_1(n)$ are, therefore, not bandlimited, and their decimation results in aliasing. To cancel the aliasing effect generated by the analysis filter bank, the filter pair in synthesis bank can be chosen as

$$F_0(z) = H_1(-z), \qquad F_1(z) = -H_0(-z) \tag{2.2}$$

The reason is stated below [4]. From Figure 2.3,

$$X_k(z) = H_k(z)X(z) \qquad k = 0,1 \tag{2.3}$$

The z-transform of the decimated signals $v_k(n)$ are

$$V_k(z) = \frac{1}{2}[X_k(z^{1/2}) + X_k(-z^{1/2})] \qquad k = 0,1 \tag{2.4}$$

And the z-transform of $Y_k(z)$ is $V_k(z^2)$. Therefore,

$$Y_k(z) = V_k(z^2) = \frac{1}{2}[X_k(z) + X_k(-z)] \tag{2.5}$$

$$= \frac{1}{2}[H_k(z)X(z) + H_k(-z)X(-z)] \qquad k = 1,2$$

The output then can be written as

$$\hat{X}(z) = F_0(z)Y_0(z) + F_1(z)Y_1(z) \tag{2.6}$$

$$= \frac{1}{2}[H_0(z)F_0(z) + H_1(z)F_1(z)]X(z) + \frac{1}{2}[H_0(-z)F_0(z) + H_1(-z)F_1(z)]X(-z)$$

The last term above represents aliasing. If the filter pair in synthesis bank is chosen such that the following holds:

$$H_0(-z)F_0(z) + H_1(-z)F_1(z) = 0 \tag{2.7}$$

then the aliasing effect generated by the analysis bank is eliminated.

2.3. MAPPING BETWEEN FREQUENCY DISTRIBUTION AND BAND DISTRIBUTION

The output of the full tree PWT decomposition is an N-band array, where

$$N = 2^L \tag{2.8}$$

L is the number of decomposition level. For example, a 2-level PWT decomposition will generate a 4-band array of data (lowpass-lowpass, lowpass-highpass, highpass-lowpass, highpass-highpass.) Which means that the input signal is decomposed into 4 frequency bands.

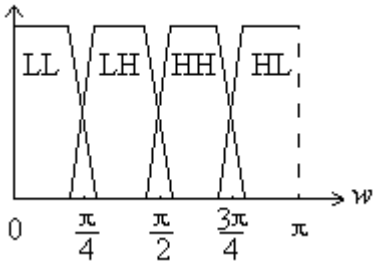

Figure 2.4 Frequency Response of 4-Band PWT Decomposition

However, the mapping between these bands to the corresponding frequency is not direct. From Figure 2.4, LL band maps to [0 $\frac{\pi}{4}$], LH band maps to [$\frac{\pi}{4}$ $\frac{\pi}{2}$], whereas HL band maps to the highest frequency [$\frac{3\pi}{4}$ π], HH band

maps to the 2nd highest frequency [$\frac{\pi}{2}$ $\frac{3\pi}{4}$]. This mapping is caused by the downsampler. When a signal is downsampled by 2, it can be viewed as having its frequency range expanded from [0 π] to [0 2π]. The frequency component that is originally located at π/N is then mapped to 2π/N. Furthermore, if this component is originally in [$\frac{\pi}{2}$ π] (i.e. in highpass band) after downsampling, 2π/N is in the range of [π 2π] and it needs to be mapped back to the range [0 π] by the rule:

$$f_{ouput} = \pi - (f_{input} - \pi) \tag{2.9}$$

A numerical example can be found in [5].

2.4. WAVELET BASIS FAMILIES

There are a very large number of PWT basis functions. The group we have selected to implement in the de-nosing software of the VSAE represents a healthy cross section and includes the following six wavelet families: Daubechies, Coiflet, Symlets, Bi-orthogonal, Beylkin, and Vaidyanathan. Their characteristics vary according to several criteria:

1. Support of ψ and ϕ in Equation (2.1) and their Fourier transforms: the speed of convergence at infinity to 0 of these functions when the time and the frequency goes to infinity, which quantifies both time and frequency localizations.
2. Symmetry, a key property to avoid phase distortions in image processing.
3. Number of vanishing moments for ψ or for ϕ (if it exists). If a wavelet has *n* vanishing moments, the wavelet transform can be interpreted as a multiscale differential operator of order *n*. This yields the relation between the differentiability of a signal and its wavelet transform decay at fine scales, which is useful for compression purposes.
4. Regularity, which is useful for getting nice features such as smoothness of the reconstructed signal or image.

Table 2.1 provides a summary of these criteria for the different wavelet families and Table 2.2 gives the relationship between Bi-orthogonal filter names and the actual support of the associated filters.

Table 2.1 Criteria in Different Wavelet Families.

Name	Order *N*	Filter length	Symmetry	Vanishing Moments for ψ (ϕ)
Daubechies	$N > 0$	$2N$	Far from	N
Coiflet	$N = 1, 2, \ldots, 5$	$6N$	Near from	$2N$ ($2N$-1)
Symlets	$N = 2, 3, \ldots, 8$	$2N$	Near from	N
Bi-orthogonal	$N_r.N_d$	See Table 2.	Yes	N_r-1
Beylkin		18	Far from	
Vaidyanathan		24	Far from	

Table 2.2 Map of Biorthogonal Filter Names to Associated Filter Support

Name $N_r.N_d$	Decomposition filters length	
	Lowpass	Highpass
1.1	2	2
1.3	6	2
1.5	10	2
2.2	5	3
2.4	9	3
2.6	13	3
2.8	17	3
3.1	4	4
3.3	8	4
3.5	12	4

3.7	16	4
3.9	20	4
4.4	9	7

2.5. RECONSTRUCTION PROPERTIES

According to [6], perfect reconstruction for a DFB means that the output is a delayed and possibly scaled version of the input.

$$\hat{X}(z) = cz^{-k}X(z) \tag{2.10}$$

Furthermore, if the following term from Equation (2.6) satisfies the relationship:

$$H_0(z)F_0(z) + H_1(z)F_1(z) = 2I \tag{2.11}$$

the output will be exactly equivalent to the input. This is called perfect reconstruction.

2.5.1. Validation of Perfect Reconstruction Using Vehicle Signals

Although, perfect reconstruction is conceptually a very nice result, the realities of numerical implementations imply that residual errors of some magnitude are to be expected. For purposes of examining what order of magnitude residuals would result we took a vehicle signal, decomposed it using the PWT and reconstructed it using the inverse PWT. The error between the original vehicle signal and the reconstructed vehicle signal was calculated. The error was measured in the L_2 sense. This measurement norm is specified as follows:

$$L_{2err} = \sqrt{(\hat{x}_1 - x_1)^2 + (\hat{x}_2 - x_2)^2 + \cdots + (\hat{x}_n - x_n)^2}\ . \tag{2.12}$$

Where the original signal is given as the series $[x_1, x_2, \cdots, x_n]$ and the output signal after decomposition, reconstruction and time registration is $[\hat{x}_1, \hat{x}_2, \cdots, \hat{x}_n]$. The vehicle signal used is given in Table 2.3.

Table 2.3 Vehicle Signal Used in Verification of the Numerical Accuracy of Perfect Reconstruction

Test Signal: T-62 Battle Tank, Speed 30 kph, CPA: 75 meters, (ATC_2081.ad, channel A, 89088 samples)
Original Signal: $[x_1, x_2, \cdots x_n]$
Decomposed - Reconstructed Signal: $[\hat{x}_1, \hat{x}_2, \cdots \hat{x}_n]$
L_2 norm error = $\sqrt{(\hat{x}_1 - x_1)^2 + (\hat{x}_2 - x_2)^2 + \cdots (\hat{x}_n - x_n)^2}$

Prior to comparing the reconstructed signal to the original signal the proper accounting is performed to eliminate the overhead associated with the convolution of the PWT filters that artificially pad the front and back end of the reconstructed signal. Table 2.4 gives an example of the numerical error residuals observed due to the PWT perfect reconstruction algorithm (i.e. the inverse PWT operation). This experiment was performed across all six PWT family basis functions implemented in the VSAE. The results exhibited the same trends and approximately the same order of magnitude of error residuals as shown in Table 2.4.

Table 2.4 Typical Error Residuals Observed Using PWT Signal Reconstruction

Basis Family: Symlets							
Length Level	**4**	**6**	**8**	**10**	**12**	**14**	**16**
1	0.01608	0.02064	0.02386	0.02314	0.02809	0.02862	0.02864
2	0.02717	0.03180	0.03976	0.03333	0.04346	0.04305	0.04096
3	0.03436	0.04486	0.05173	0.04109	0.05641	0.05559	0.04984
4	0.04108	0.05593	0.06441	0.04786	0.06918	0.06782	0.05772
5	0.04758	0.06675	0.07560	0.05351	0.08235	0.07960	0.06476
6	0.05481	0.07537	0.08928	0.05916	0.09473	0.09097	0.07158
7	0.06078	0.08648	0.09933	0.06430	0.10628	0.10187	0.07728

The conclusions to be drawn from this experiment are as follows:

1. The L_2 norm error between the original signal and the decomposed-reconstructed signal is very small. The possible reasons of the finite error values are the limited numerical resolution of the filter coefficients and the rounding during convolution.
2. The L_2 norm error increases as the decomposition-reconstruction level increases. This is expected, the greater the decomposition length in terms of additional DFB with each level the greater the number of calculations and the more susceptible the result to round-off error.
3. The longer the signal, the bigger the L_2 norm error. Once again this directly correlates to greater number of calculations.
4. L_2 norm error is however not sensitive to the change in filter support. This is observable directly in Table 2.4 by noticing that their exists no strong trend in any specific given row. This general trend was observed for all six basis families.

2.6. PACKET WAVELET TRANSFORM (PWT) BASED DE-NOISING

The most common de-noising methodology is averaging. Although averaging can reduce the noise effect, some finer details of the signal are also removed by averaging. The averaging process inherently prevents a maximum preservation of signal information and more closely resembles a low pass filtering operation. Figure 2.5 gives a comparison between wavelet de-noising and averaging. It shows that in wavelet de-noising, although the noise attached to the signal is removed, the finer detail is kept after de-noising. The wavelet transform has an interesting property that makes it suitable for de-noising. After decomposition, the number of coefficients with significant energy is small. However, the signal can be accurately represented by these coefficients. By applying a proper threshold to all coefficients, these significant energy coefficients can be extracted. The rest of the coefficients are treated as noise and are removed. It is has been shown that the de-noising performance of the PWT is superior to that obtainable by the Discrete Wavelet Transform (DWT) [1].

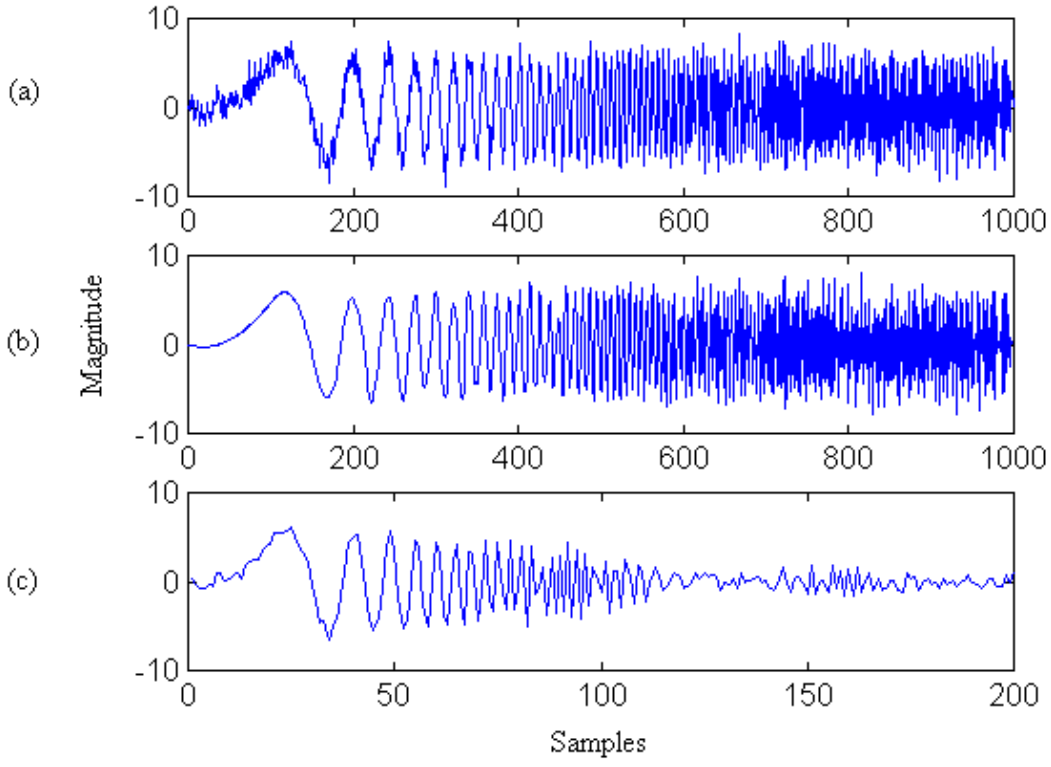

Figure 2.5 Comparison between Wavelet De-noising and Averaging. (a) Chirp Signal Corrupted with Noise, (b) Signal after Wavelet De-noising, (c) Signal after Averaging

2.6.1. PWT De-noising Principles

The key principle of PWT de-noising is to utilize the idea that based on the correlation of the input with the decomposing basis function, the transformed coefficients maybe large (high correlation) or small (low correlation). These small coefficients are possibly generated from the noise that is embedded in the signal. If a proper threshold can be found, some thresholding method can be applied to separate the noise from the signal. Two properties of the PWT contribute to separating the signal and noise components [1]. The first property is that, by properly choosing transformation parameters such as basis, support and level, the decomposition data will contain relatively few significant coefficients. The second property is that, if an input signal is a white noise, the transformed data will also be white. Therefore, the noise contained in an input signal will generate noisy coefficients (small) contributing to all coefficients in all bands. However, the typical characteristics of a signal transformation are to concentrate the PWT coefficients among a relatively few number of coefficients that will generally be large in their respective bands of distribution. The exact characteristics of this process are of course dependent on the type of signal being transformed. It is this precise difference between the transform characteristics of noise sources verses signal sources that permits the opportunity to provide separation via the application of an appropriate thresholding scheme on the transformed data.

The PWT based de-noising procedure can be summarized as follows:

1. Decompose the input signal with suitable parameters using PWT.
2. Suppress the noisy coefficients by non-linear thresholding methods.
3. Reconstruct the signal using the inverse PWT.

2.6.2. Noise Estimators

Based on the discussion in the previous section, the best threshold to separate the noise and the signal should be larger than all noisy coefficients and smaller than all signal coefficients. In this way, all noisy coefficients are removed and all signal coefficients are retained. However, since it is not possible to tell which coefficients are attributable to noise sources verses those coefficients attributable to the signal source, the calculation of the threshold should be based on the statistical properties of the transformed coefficients. The transformed coefficients in each band can be written as the noise corrupted observation signal *y(n),* where *y(n*) is defined as:

$$y(n) = f(n) + \sigma z(n) \quad n = 1,2,\ldots \tag{2.13}$$

The term *f(n)* is the deterministic function to be estimated and z*(n)* is an independent, identically distributed, normal random variable with mean equal to zero and variance equal to one. The term σ is the standard deviation of the noise. At higher frequency bands, where there are a considerable number of coefficients in each band, the signal *f(n)* is assumed to be sparse, this is the rational for estimating the noise variance σ^2 from this portion of the data. From [7], a robust estimator is applied:

$$\hat{\sigma}^2 = med(abs(y(1), y(2), \cdots)) / 0.6745 \tag{2.14}$$

where *med(abs(…))* denotes the median of the absolute value of a series, and the factor 0.6745 is chosen for calibration with the Gaussian distribution. The above noise estimator can be applied to the input signal with either color or un-scaled white noise. If the signal contains color noise, after decomposing into bands, Equation (2.14) is applied to each band to calculate the band-dependant noise estimator. If the signal contains un- scaled white noise, the highest frequency band is used to calculate the noise estimator for all bands. The noise estimator acts as a scaling factor for the threshold value applied to each band. Figure 2.6 gives a schematic of the scaling application.

2.6.3. Threshold Selection

Four types of thresholding methods are introduced in this section: Universal, SURE, Hybrid, and Minimax.

2.6.3.1. Universal Threshold T_U

$$T_U = \sqrt{2\log n} \quad n \text{ is number of coefficients available at the output of a specific band} \tag{2.15}$$

Universal threshold is a conservative choice from certain theoretical perspectives. If the $Z_1, Z_2, \ldots, Z_n$ are normally distributed random variables with zero mean and variance σ_i^2, then

$$P(\max_{1 \le i \le n} |Z_i / \sigma_i| > T_U) \to 0 \text{ as } n \to \infty \tag{2.16}$$

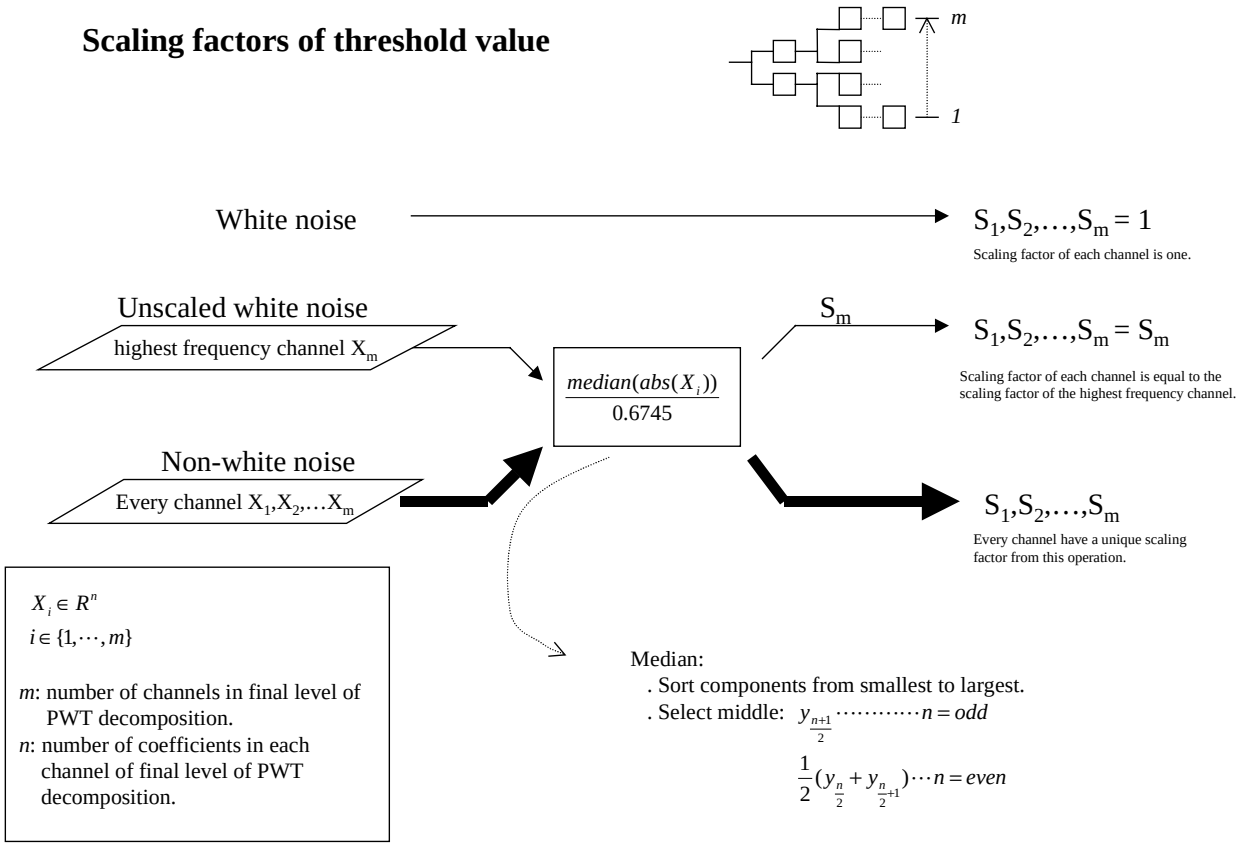

Figure 2.6 Scaling Factor of Threshold Value

whether or not the variables are independent [7]. Equation (2.16) indicates that in the limit of large sample size *n*, no elements Z_i/σ_i will have magnitude greater than the quantity T_U. That is, the possibility of the noise passing the threshold T_U is very small.

2.6.3.2. SURE Threshold T_S

SURE stands for Stein's Unbiased Risk Estimate. It was proposed by Donoho and Johnstone [8] and is based on the work of Stein [9] in the area of multivariate normal distributions. It is a data based threshold choice obtained by minimizing the estimated mean square error (risk) for threshold value over the range [0 $\sigma\sqrt{2\log n}$] [7]. Compared to the Universal threshold, it performs better in terms of L_2 loss because of smaller thresholds.

2.6.3.3. Hybrid Threshold T_H

SURE is a data based threshold choice, it is known to perform poorly in the low SNR region. The threshold estimate is biased and thus produces an unsuitable threshold because the noise dominates the signal in transformed coefficients. Hybrid is a mixture of Universal and SURE. It chooses between T_U and T_S based on the SNR. If the SNR is very small, and T_S performs poorly, T_U will be chosen instead [8].

2.6.3.4. Minimax Threshold T_M

Minimax is a data independent threshold. It is designed to select the choice of estimators that minimizes the risk (maximum mean square error) of the input signal. The application of this method to wavelet based thresholding was also proposed by Donoho and Johnstone [10]. The numerical formula used is:

$$T_M = 0 \qquad for \quad n \le 32$$
$$T_M = 0.3936 + 0.1829 * \log_2 n \qquad for \quad n > 32 \tag{2.17}$$

Compared to other thresholds, T_M performs poorly in the low SNR range which is a similar to the performance of the SURE (i.e. T_S) threshold in the low SNR area.

2.6.4. Thresholding Methods

Two methods for applying the thresholds to suppress or modify the coefficients of the decomposition are discussed in this section. They are known respectively as hard thresholding and soft thresholding. The relationship between the inputs and outputs of both methods are illustrated in Figure 2.7.

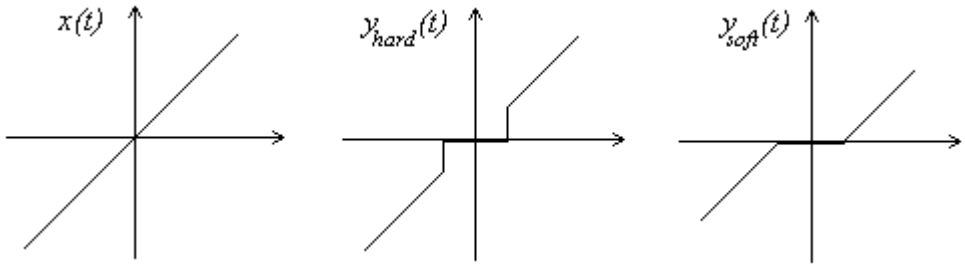

Figure 2.7 Input vs. Output of Hard and Soft Thresholding Application

The outputs of the respective hard and soft thresholding methods using a generic threshold *T* are defined as follows:

$$y_{hard}(t) = \begin{cases} x(t), & |x(t)| > T \\ 0, & |x(t)| \le T \end{cases} \tag{2.18}$$

$$y_{soft}(t) = \begin{cases} sign(x(t))(|x(t)| - T), & |x(t)| > T \\ 0, & |x(t)| \le T \end{cases}$$

In the hard thresholding method, coefficients exceeding the threshold *T* are retained while the others are set to zero. One potential side effect of this process is that the removal of all fine detail from the signal may produce undesired spikes in the reconstructed signal. In the soft thresholding method, instead of just zeroing out the coefficients that are smaller than the threshold *T*, the magnitude of all other coefficients are reduced by the amount of *T*. This method can avoid the undesired spikes that may be produced by hard thresholding. However, since all coefficients are modified, the signal shape may be distorted. It is especially obvious for signals with low SNR.

2.7. SOFTWARE IMPLEMENTATION OF PWT DE-NOISING METHOD

2.7.1. Architecture

In order to perform the experiments and have an initial permanent home for this preprocessing method, the PWT was integrated into our object-oriented Vehicle Signal Analysis Environment (VSAE). Its specific implementation closely parallels the architecture used to implement the Continuous Wavelet Transform (CWT) object software in the VSAE. A PWT object is created when the PWT view is generated via the user electing to use this computational option from the menu item of the mainframe of the VSAE. All operations that are not related to viewing the PWT view, such as the numerical operations of decomposition, de-noising, reconstruction … etc, are done in the PWT object. The PWT view is the user interface GUI that receives commands from a user and sends them to the PWT object for processing. A de-noised /reconstructed dialog will pop up whenever a PWT data de-noising or reconstruction operation is requested. The purpose of the pop-up dialog is to provide a de-noised or reconstructed view where the user can compare it with the PWT view or the original signal main view respectively before electing to replace the original data with the processed data.

2.7.2. PWT I/O and Processing Operations Under the VSAE

The PWT object gets the input data from the signal object attached to the signal main view that invoked the PWT operation. Like the CWT object class, the PWT object class is declared as a friend class to the signal object class so that it can access its private data. The PWT object can process the whole data or just part of the data according to the starting and ending points defined by the user in the original signal object. After processing, the

object sends a copy of the PWT data to the PWT view. The view can modify that copy depending on whether the user selects to view the PWT data in signed components, magnitude or dB format. If the de-noising or reconstruction process is selected via the processing controls available to the user in the PWT view, a copy of the de-noised or the reconstructed data is then sent to the de-noised/reconstructed dialog which then pops up in the VSAE. The user then has the opportunity to compare the PWT data or signal time domain data before and after de-noising. If the result is acceptable, the user can elect to update the signal object by replacing the original data with the de-noised data. Figure 2.8 illustrates the architecture and I/O of PWT view, object and dialog.

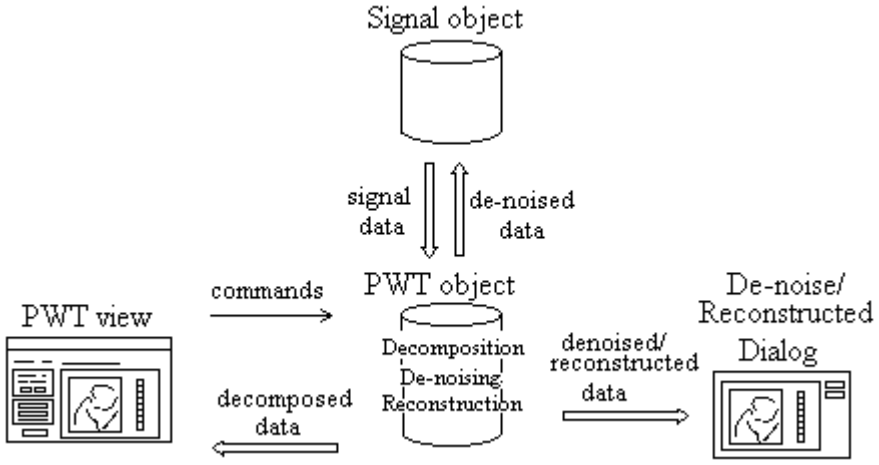

Figure 2.8 Architecture and I/O of PWT View, Object and Dialog

2.7.3. The PWT User Interface Under the VSAE

Figure 2.9 shows an example of the PWT interface under the VSAE. The PWT shown in the 2D color display, is a de-noised version of the tank transporter (MAZ537-G, file: Atc_2104.ad, channel B) vehicle signal. The 2D display is shown in the truncated magnitude mode to highlight for the user a view of the data which facilitates seeing the strongest PWT components. The particular decomposition used was the Biorthogonal Basis 3.5. The level of decomposition is 8. The scale axes of the 2D projection is arranged in frequency mode. The type of de-nosing performed involved using the SURE threshold applied using the Hard Thresholding method.

2.8. INITIAL INVESTIGATION INTO THE USE OF THE PWT DE-NOISING METHODS APPLIED TO VEHICLE SIGNALS

The following sections provide an initial investigation into the use of the PWT de-noising methods applied to vehicle signals through the use of empirical sensitivity studies. The techniques developed and capabilities integrated into the VSAE represent a rich source of discrete wavelet basis functions, decomposition/reconstruction options and nonlinear noise removal processing options. In configuring a preprocessing or equivalently a de-noising strategy, a number of questions surface such as:

1. Which discrete wavelet basis function is best for the vehicle signal domain?
2. What is the effect of increasing basis support?
3. What role, if any, does the decomposition and reconstruction length play?
4. Are there any advantages to orthogonal versus biorthogonal decompositions?
5. Which set of nonlinear processing strategies are most beneficial to the vehicle signal domain (i.e. Universal, Hybrid, Minimax, SURE, etc.)?
6. Does the nonlinear processing implementation make any difference (i.e. Hard thresholding versus Soft thresholding)?

In an attempt to address these sort of questions for the vehicle signal domain, a set of sensitivities studies was conducted on these various PWT de-noising parameters with respect to the vehicle signals. The underlying goal of the studies is to have a least one set of data which can be examined for determining effective combinations of parameter choices for use in a PWT vehicle signal de-noising preprocessor.

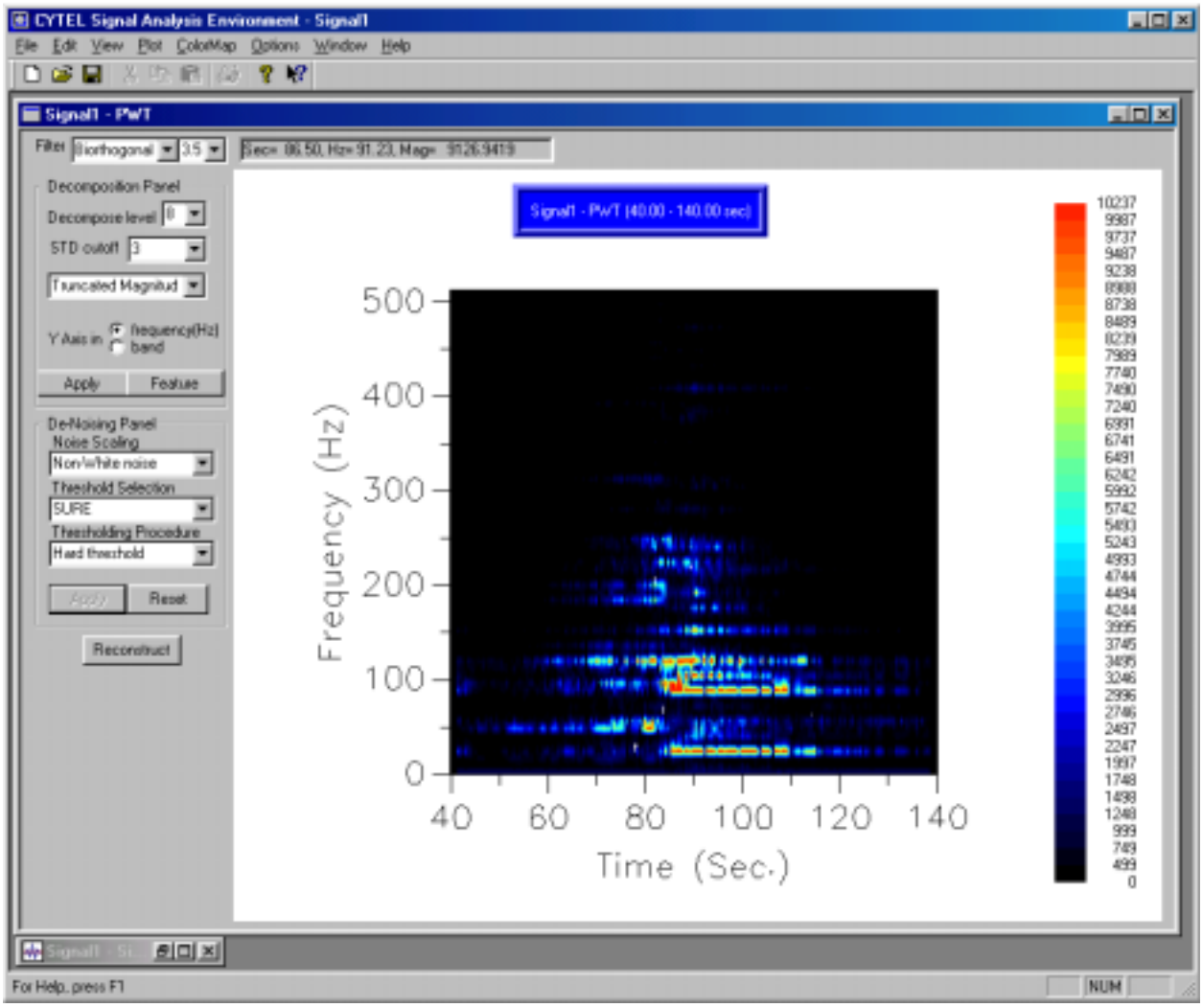

Figure 2.9 PWT Interface under the VSAE

2.9. TEST SIGNALS USED IN THE STUDY

Two signals are used in the experiments:

1. The first signal is modeled from channel A of vehicle signal file: Atc2009.ad. A total of 1500 samples are taken from the high SNR region of the vehicle signal Atc2009. These samples are then used to construct a parametric based ARMA model of the vehicle sequence. The result is an IIR filter whose impulse response matches exactly the vehicle sequence for the first *N+1* samples where *N* is the numerator order of the model. This model is implemented using Matlab's Signal Toolbox "*prony* method" to generate the numerator and denominator coefficients [13]. The length of numerator and denominator of the IIR filter are 1024 and 256 respectively. An impulse of length 1501 samples is used to drive the model and generate a modeled vehicle signal length of 1501 samples.
2. The second signal is a chirp signal. The signal length is 1024 samples. Unlike the vehicle signal, the frequency response spreads across the entire frequency range. This signal is used as a comparison to the test signal 1 for only one sensitivity study. That particular sensitivity study examines the sensitivity of choosing varying levels for decomposition-reconstruction of signals during de-noising.

2.10. TEST PROCEDURE

The test procedure is shown in Figure 2.10. A test signal is corrupted with scaled white noise to generate a noisy signal with different SNR values. The noisy signal is then processed by the PWT de-noising tool implemented

in the VSAE. The L_2 norm error between the de-noised signal and the test signal (without noise) is used as an indicator of how well the de-noising tool performs. Tests 1 through 4 use the modeled vehicle signal as input. Test 5 conducts sensitivity studies performed on both the modeled vehicle signal and the chirp signal.

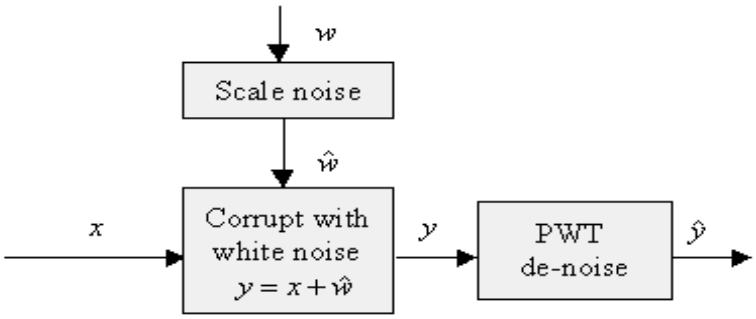

Figure 2.10 Test Procedure

2.11. TEST 1: SENSITIVITY OF DIFFERENT THRESHOLDING METHOD

Parameters for decomposition-reconstruction and de-noising
Wavelet basis: Daubechies 10
Decomposition-reconstruction level: 5
Noise source: Un-scaled white noise
Thresholding value selection: Universal

Table 2.5 L_2 Norm Error for Different Thresholding Methods

SNR (dB)	-10	-3.0103	1	5	10	20
Hard thresholding	64.9897	36.3622	30.3071	22.4132	18.8181	13.0927
Soft thresholding	44.2898	37.1119	34.8372	29.7497	25.7482	20.6010

Table 2.5 indicates that hard thresholding has smaller L_2 norm error than soft thresholding except for in the case where the SNR equals –10 dB. Due to the better performance of hard thresholding over the SNR region of most interest (i.e. over the range SNR: 1 dB to 20 dB), the rest of the experiments are conducted using the hard thresholding method.

2.12. TEST 2: SENSITIVITY OF DIFFERENT THRESHOLD VALUES

Parameters for decomposition-reconstruction and de-noising
Wavelet basis: Daubechies 10
Decomposition-reconstruction level: 5
Noise source: Un-scaled white noise
Thresholding method: Hard thresholding

Table 2.6 L_2 Norm Error for Different Threshold Values

SNR	SNR (dB)	L_2 norm error			
		Universal	Minimax	SURE	Hybrid
0.1	-10	64.9897	97.9329	115.7636	106.1397
0.5	-3.0103	36.3622	41.7729	49.9544	30.0796
1	0	30.3071	30.6777	32.9313	23.4458
5	6.9897	22.4132	18.1541	15.1689	18.0940
10	10	18.8181	14.5095	11.5225	13.4898
100	20	13.0927	8.9689	5.1135	9.8736

Figure 2.11 shows the L_2 norm error for different threshold values. For higher SNR, SURE has the smallest L_2 norm error; for middle range SNR, Hybrid has the smallest L_2 norm error; for smaller SNR, Universal

has the smallest L_2 norm error. As to the performance of Minimax, it lies between SURE and Hybrid. To reduce the number of tests, Universal and SURE thresholds are used for the rest of the sensitivity studies for the following reasons:

1. Universal threshold is data-independent while SURE threshold is data-dependent
2. Universal threshold performs best in the small SNR region while SURE threshold performs best in the high SNR region.

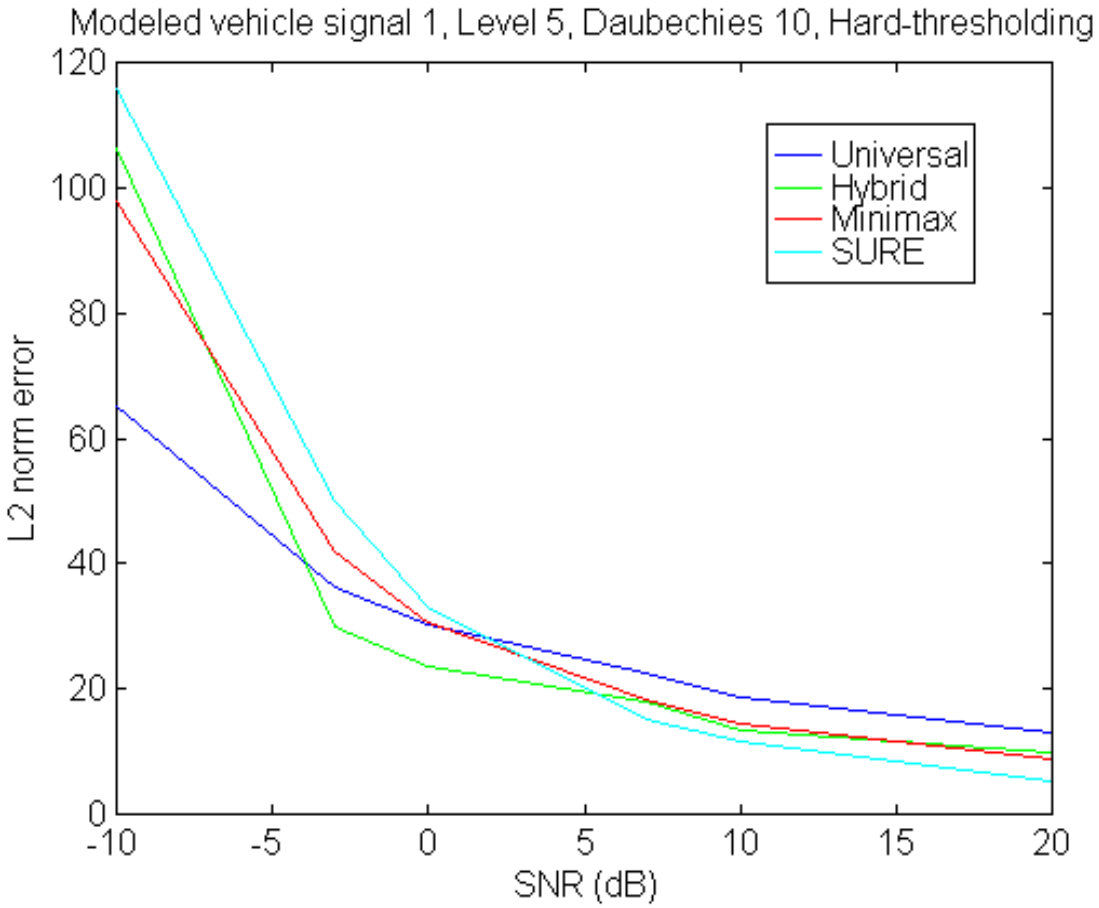

Figure 2.11 L_2 Norm Error for Different Threshold Values.

2.13. TEST 3: SENSITIVITY OF DIFFERENT WAVELET BASIS

Parameters for decomposition-reconstruction and de-noising
Filter support: 18taps. (For Symlets family, 16-tap is the longest filter.)
Decomposition-reconstruction level: 5
Noise source: Un-scaled white noise
Thresholding method: Hard thresholding
Threshold value selection: (1) Universal (2) SURE

Figure 2.12 shows the L_2 norm error for different wavelet basis. If Universal threshold is selected: for higher SNR, Beylkin and Biorthogonal have smaller L_2 norm error; for lower SNR, Daubechies and Coiflet have smaller L_2 norm error. If SURE threshold is selected: the performance of different wavelet basis is close to each other, especially in the high SNR region. However, Daubechies and Coiflet seem to perform a little better than others. Therefore, Daubechies, Coiflet, Biorthogonal wavelet basis are used for the remaining sensitivity studies.

2.14. TEST 4: SENSITIVITY OF DIFFERENT FILTER SUPPORTS

Parameters for decomposition-reconstruction and de-noising
Wavelet basis: (a) Daubechies (b) Coiflet (c) Bi-orthogonal

Decomposition-reconstruction level: 5
Noise source: Un-scaled white noise
Thresholding method: Hard thresholding
Threshold value selection: (1) Universal (2) SURE

Figure 2.13 shows the L_2 norm error for different filter support in the Daubechies family. For both Universal and SURE thresholds, Daubechies 12 performs best in the higher SNR region, and Daubechies 4 performs best in the lower SNR region. Varying L_2 norm errors do not appear to be directly related to the changing of filter support. Figure 2.13*(a)* shows that the crossover point of all filters in the family is around –5 dB. After –5 dB, those performing well in the lower SNR region start to perform worse than those performing poorly in the lower SNR region. Figure 2.13*(b)* shows that when SURE threshold is applied, the change of L_2 norm error vs. the change of filter support is more uniform than when the Universal threshold is applied. The crossover point is around 5 dB. However, the observed trend remains constant that relative good performance in the lower SNR region becomes relative poorer performance in the higher SNR region and vice versa.

Figure 2.14 shows the L_2 norm error for different filter support in the Coiflet family. Except for Coiflet 18, in both the cases where Universal and SURE thresholds are applied, the Coiflet family seems to follow the trend that in the higher SNR region, the longer the support the larger the L_2 norm error. And in the lower SNR region, the longer the support the smaller the L_2 norm error. The crossover point of applying Universal threshold is around –7.5 dB, and the crossover point of applying SURE threshold is around 7.5 dB. Coiflet 18 performs best in the SNR region lower than the crossover point. In the region higher than the crossover point, Coiflet 30 performs best.

Only 2.X and 3.X of Biorthogonal family are tested in this sensitivity study. The result is shown in Figure 2.15. From Figure 2.15, unlike Daubechies and Coiflet family, the performances of different supports are very close. There is no obvious crossover point. For both Universal and SURE scheme, in higher SNR region, except Bior 3.1, series 3.X performs better than 2.X; in lower SNR region, series 2.X performs better than 3.X. Bior 3.1 performs worst in these two series. And, Bior 2.4, 2.6 and Bior 3.3, 3.7 are the better filters in 2.X, 3.X respectively.

2.15. TEST 5: SENSITIVITY OF DIFFERENT DECOMPOSITION-RECONSTRUCTION LEVELS

In each of the following wavelet families: Daubechies, Coiflet, and Biorthogonal the two best filters of different supports are chosen to perform the test.

(I) Wavelet basis function: (a) Daubechies 6 (b) Daubechies 12
Other parameters for decomposition-reconstruction and de-noising:
Noise source: Un-scaled white noise
Thresholding method: Hard thresholding
Threshold value selection: (1) Universal (2) SURE

From Figure 2.16, and Figure 2.17, if the SURE threshold is applied, the crossover point is around 8 dB. Additionally, in the higher SNR region, the more the level the less the error; and in the lower SNR region, the more the level the more the error. However, if Universal threshold is applied, there is more than one crossover point. All of them locate between –5 dB and 0 dB. Due to the existence of multiple crossover points, there is no obvious discernible trend to follow if the Universal threshold is applied.

(II) Wavelet basis function: (a) Coiflet 18 (b) Coiflet 30
Other parameters for decomposition-reconstruction and de-noising:
Noise source: Un-scaled white noise
Thresholding method: Hard thresholding
Threshold value selection: (1) Universal (2) SURE

From Figure 2.18, and Figure 2.19, if the SURE threshold is applied, the crossover point is around 9 dB. Additionally, in the higher SNR region, the more the level the less the error; and in the lower SNR region, the more the level the more the error. However, if Universal threshold is applied, there is more than one crossover point. They locate in a large range between –7 dB and 10 dB. Due to the existence of multiple crossover points, there is no obvious discernible trend to follow if the Universal threshold is applied

(III) Wavelet basis function: (a) Biorthogonal 2.4, (b) Biorthogonal 3.3
Other parameters for decomposition-reconstruction and de-noising:
Noise source: Un-scaled white noise
Thresholding method: Hard thresholding
Threshold value selection: (1) Universal (2) SURE

From Figure 2.20, and Figure 2.21, unlike the Daubechies and Coiflet families, the Biorthogonal family has only one crossover point for both Universal and SURE thresholds. The crossover point for the Universal threshold is around 5 dB, for the SURE threshold it is around 8 dB. The trend appears to be that in the higher SNR region, the

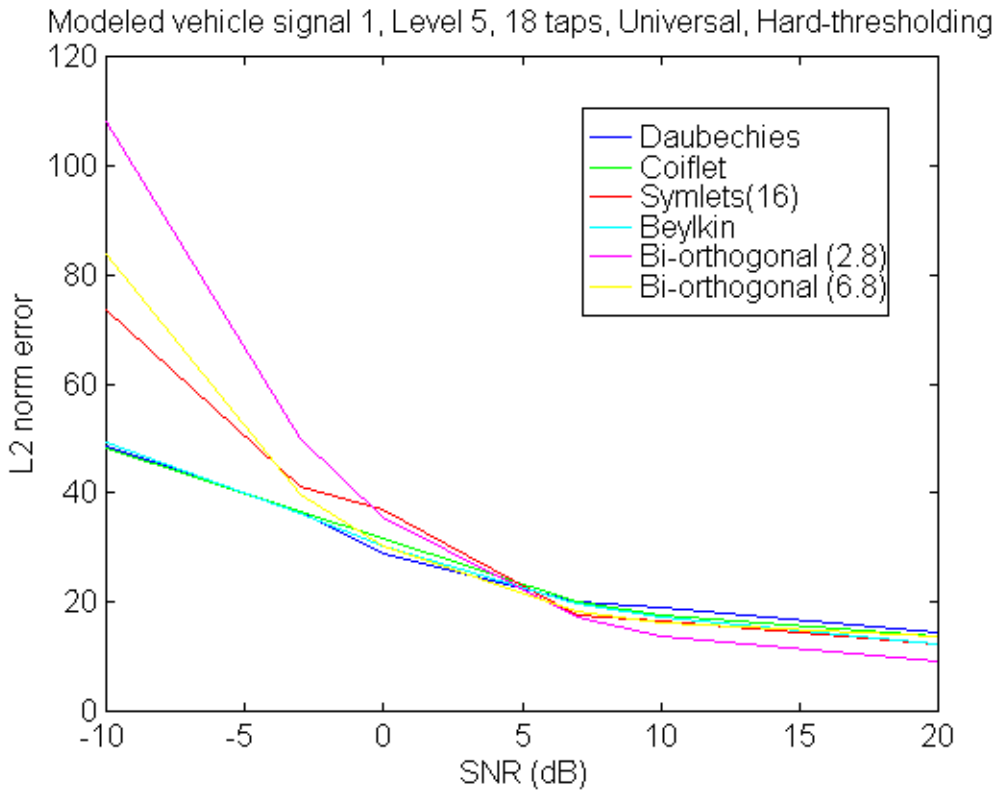

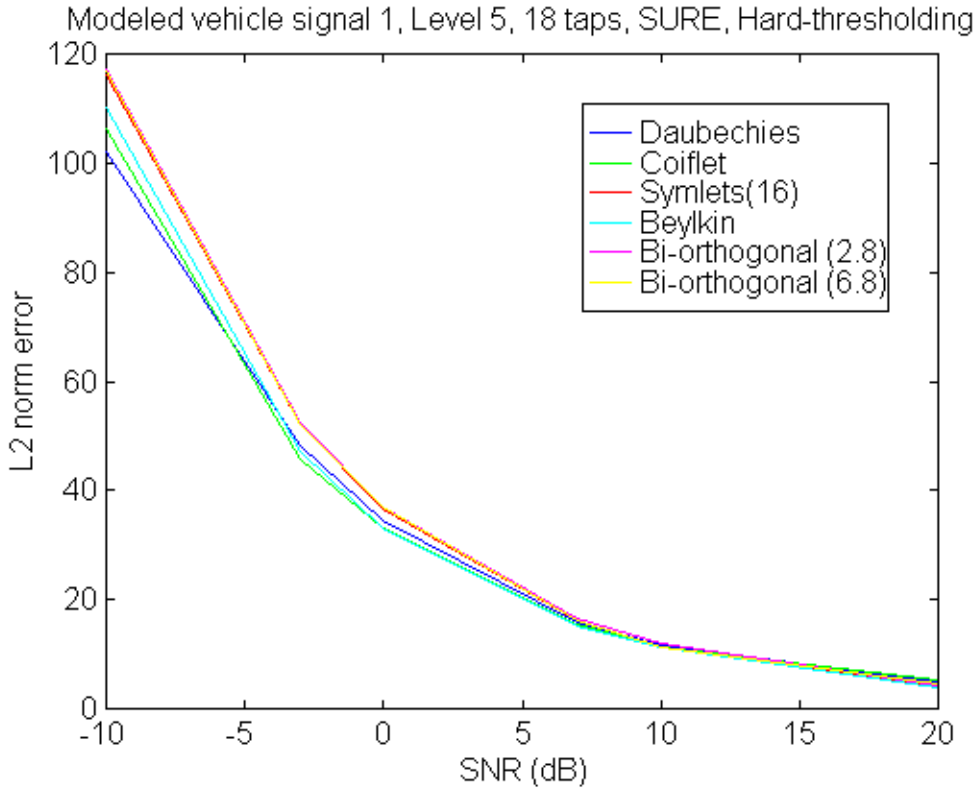

Figure 2.12 L_2 Norm Error for Different Wavelet Basis: (a) Universal, (b) SURE

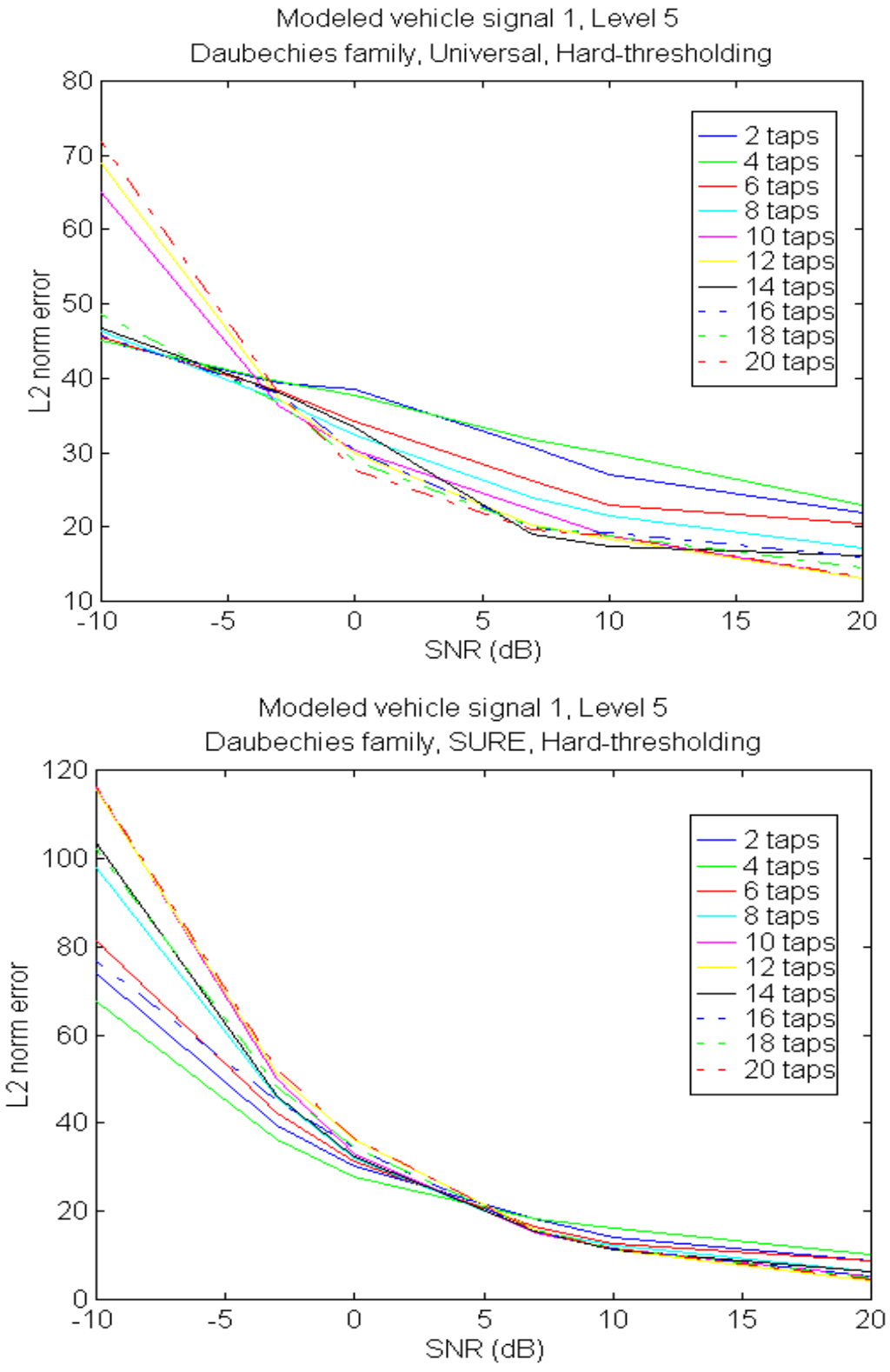

Figure 2.13 L_2 Norm Error of Different Filter Support in Daubechies Family, (a) Universal, (b) SURE Threshold is Applied.

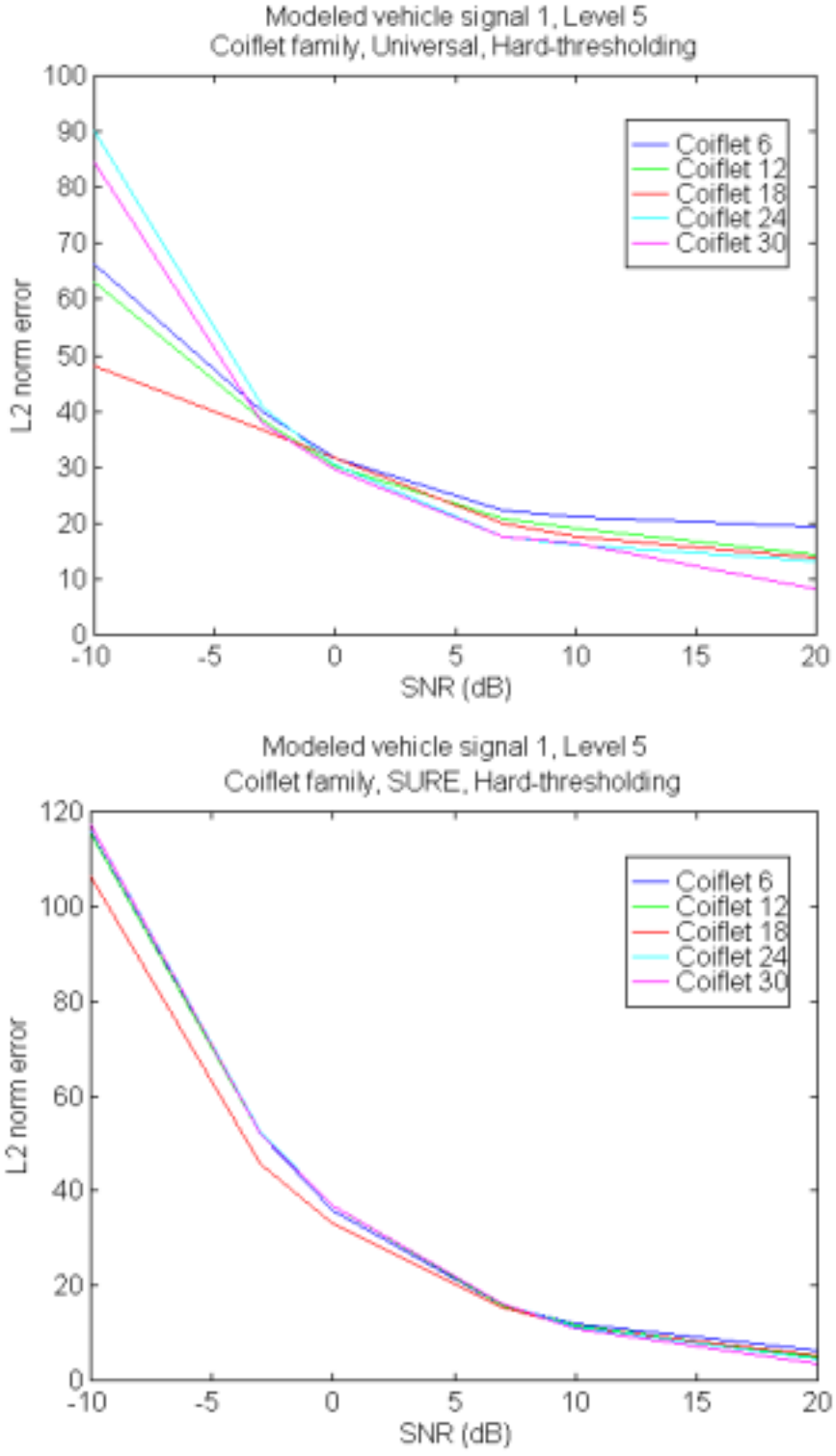

Figure 2.14 L_2 Norm Error of Different Filter Support in Coiflet family, (a) Universal, (b) SURE Threshold is Applied

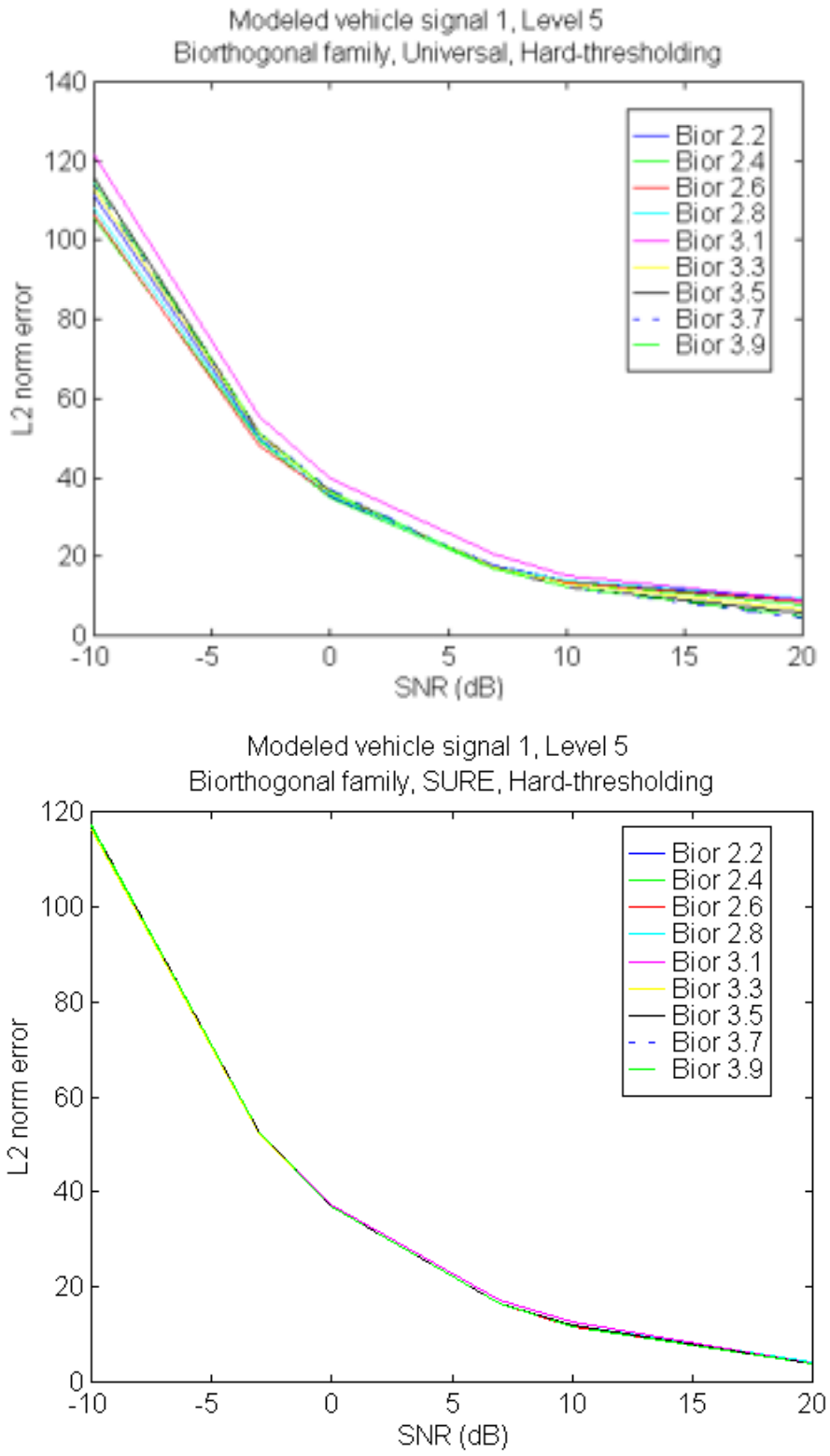

Figure 2.15 L_2 Norm Error of Different Filter Support in Biorthogonal 2.X, 3.X Family, (a) Universal, (b) SURE Threshold is Applied

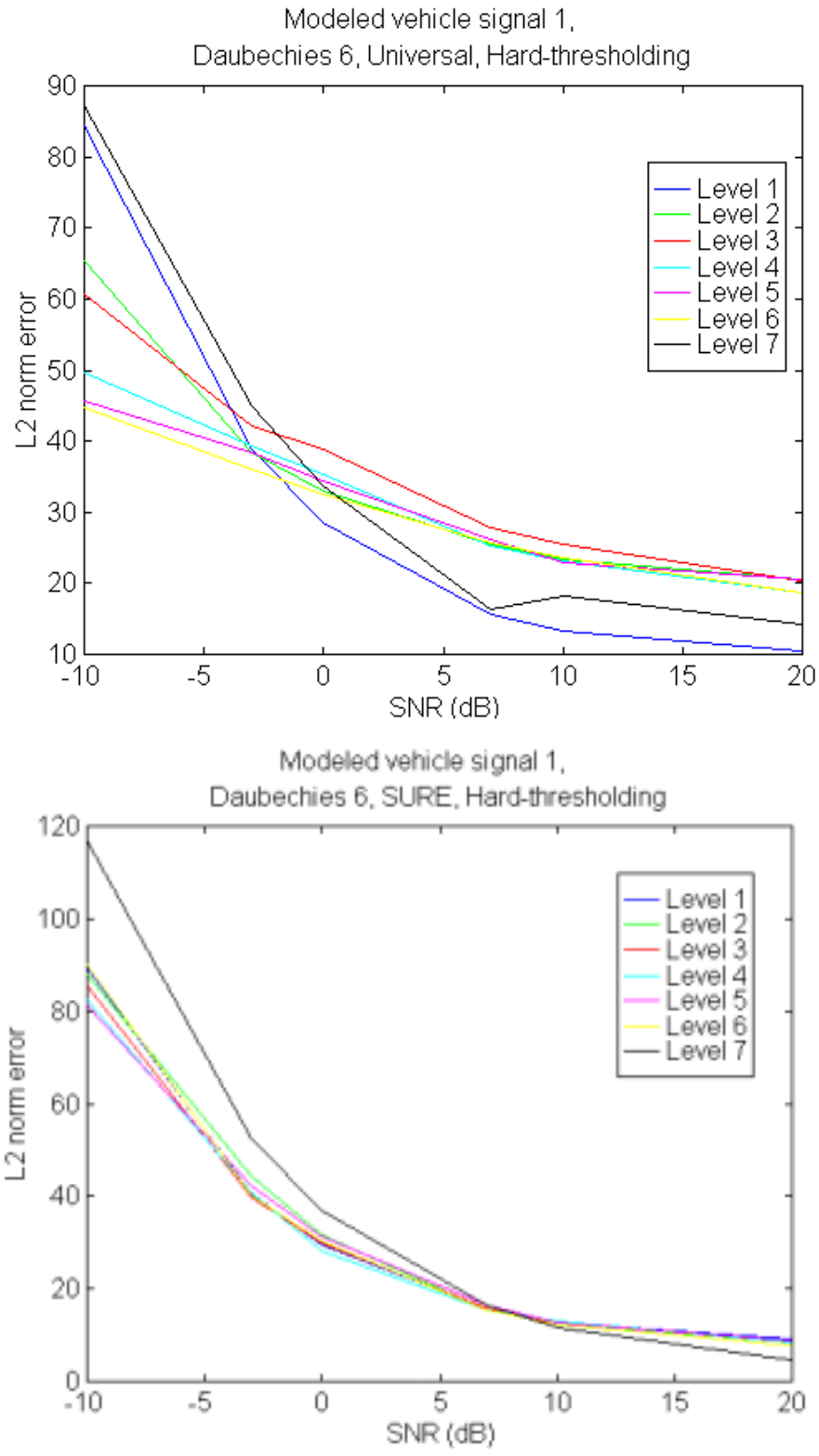

Figure 2.16 L_2 Norm Error of Different Decomposition-Reconstruction Level using Wavelet Basis Daubechies 6 (1) Universal, (2) SURE Threshold is Applied

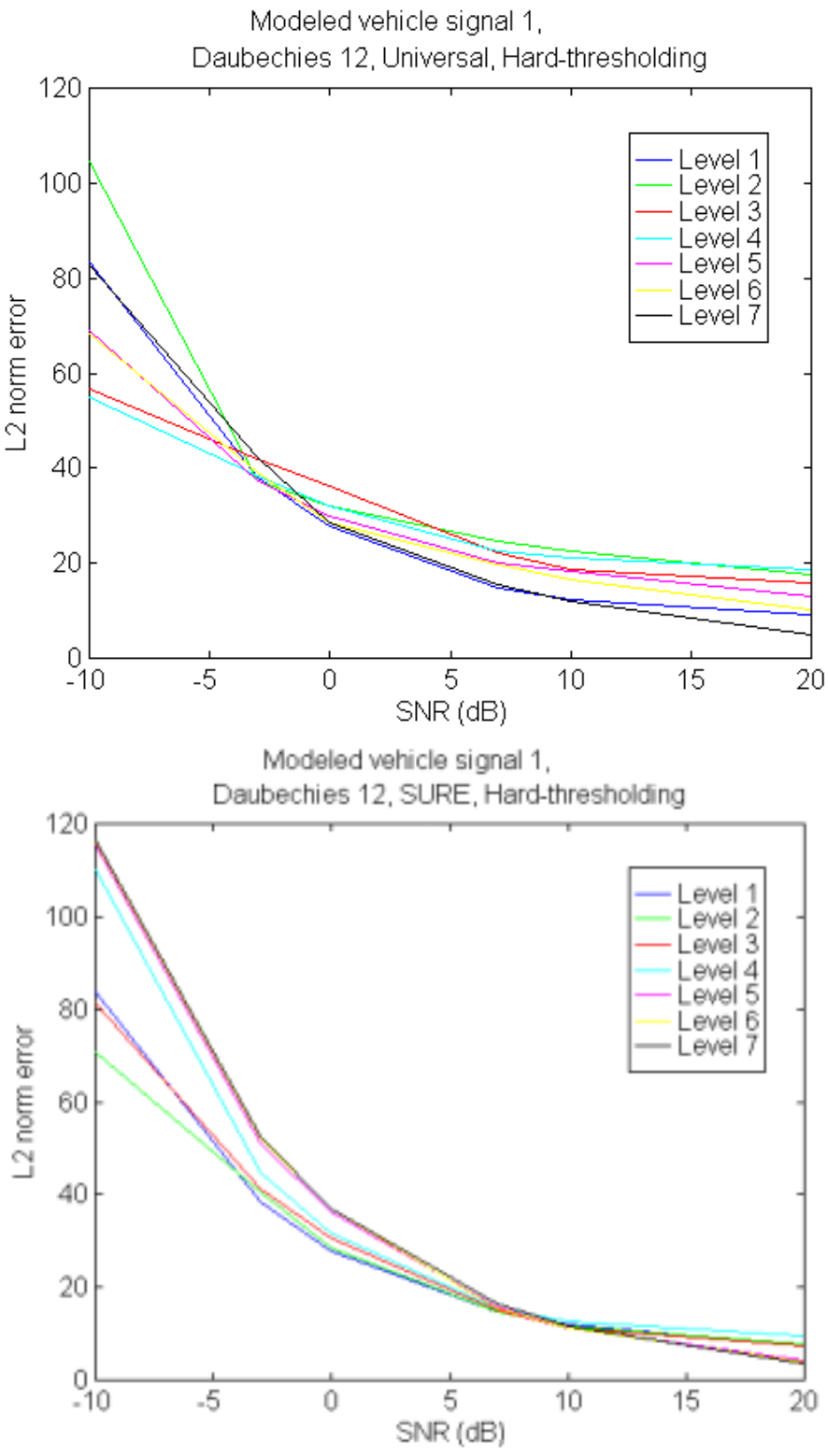

Figure 2.17 L_2 Norm Error of Different Decomposition-Reconstruction Level Using Wavelet Basis Daubechies 12 (1) Universal, (2) SURE Threshold is Applied

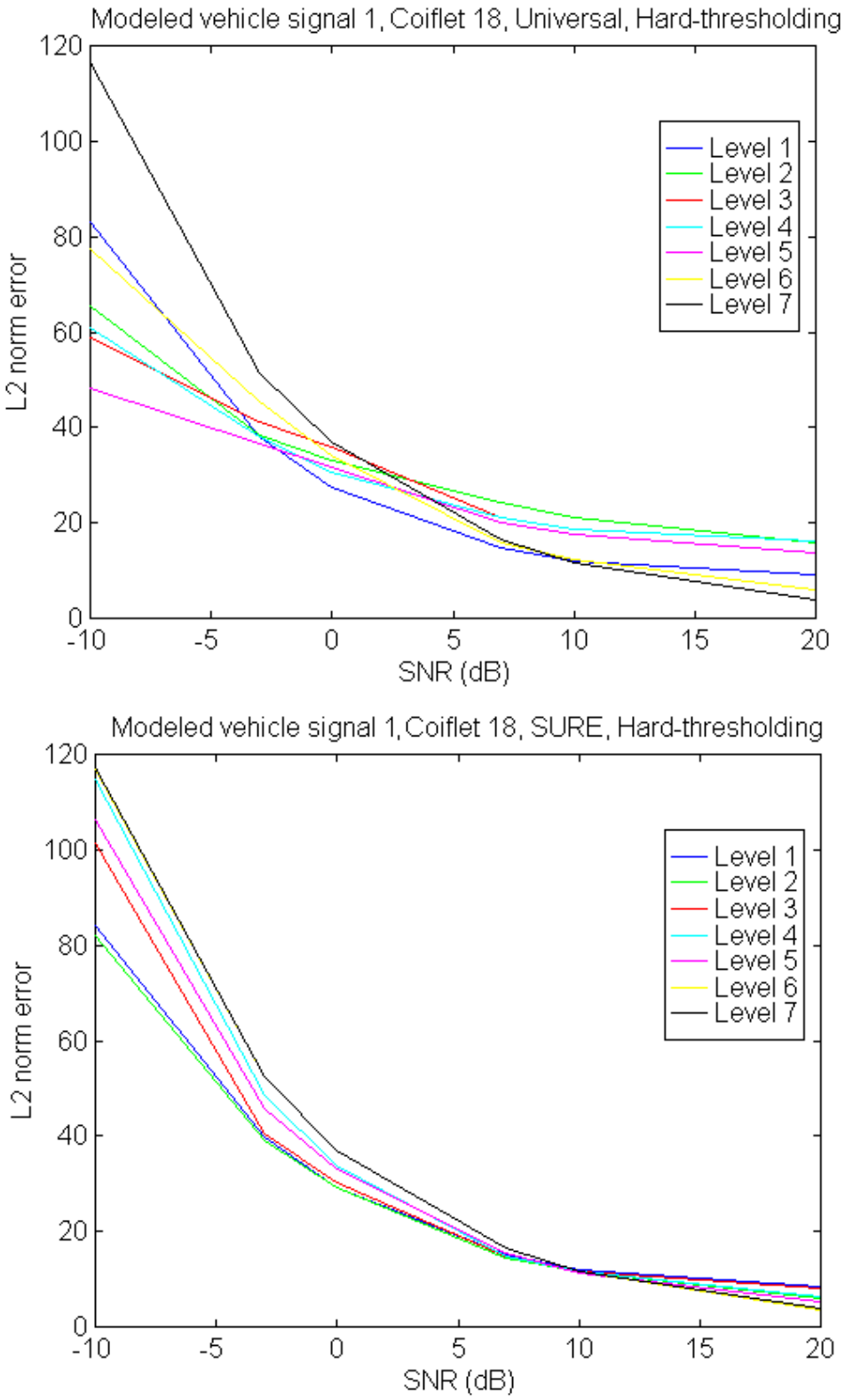

Figure 2.18 L_2 Norm Error of Different Decomposition-Reconstruction Level using Wavelet Basis Coiflet 18, (a) Universal, (b) SURE Threshold is Applied

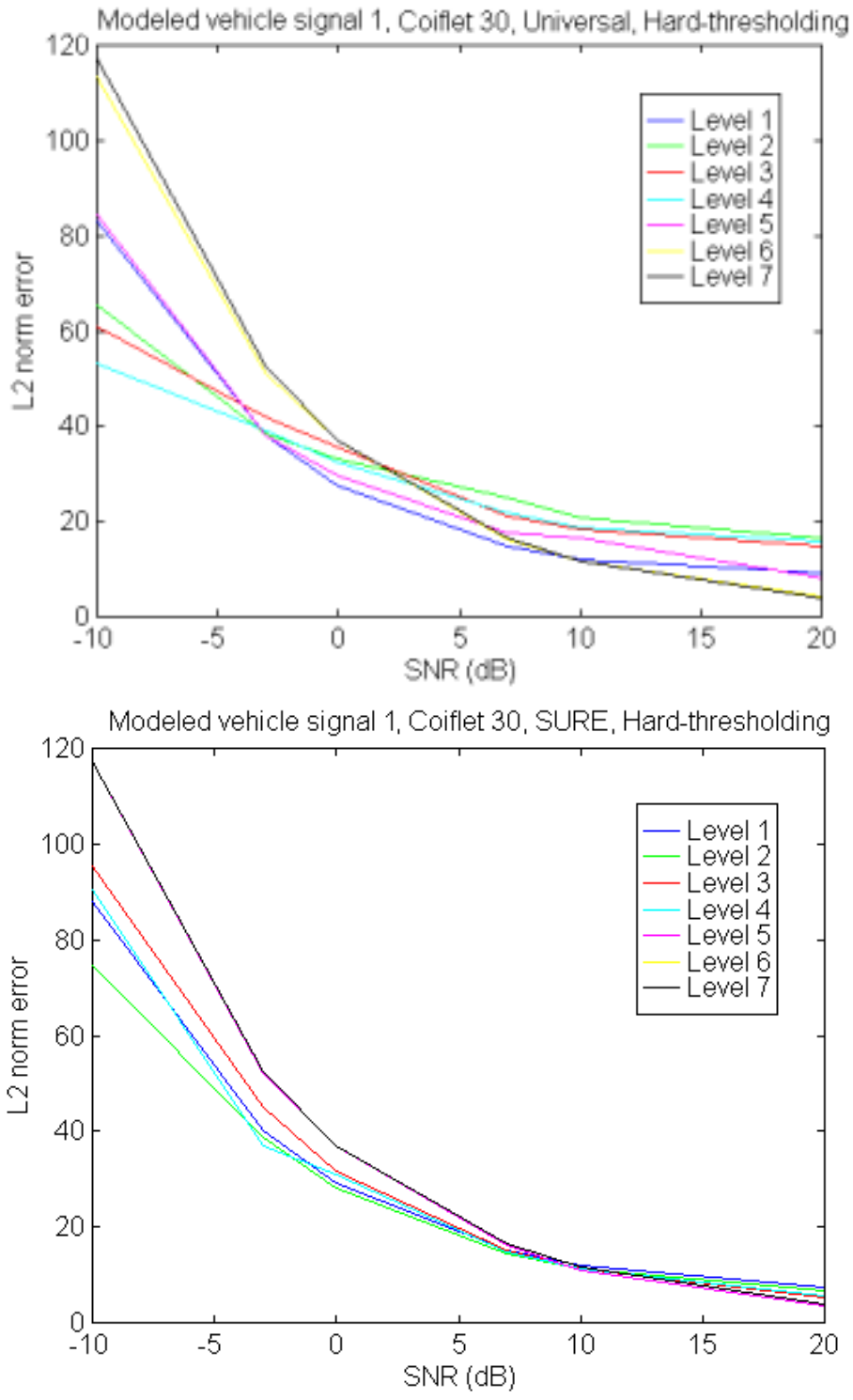

Figure 2.19 L_2 Norm Error of Different Decomposition-Reconstruction Level using Wavelet Basis Coiflet 30, (1) Universal, (2) SURE Threshold is Applied

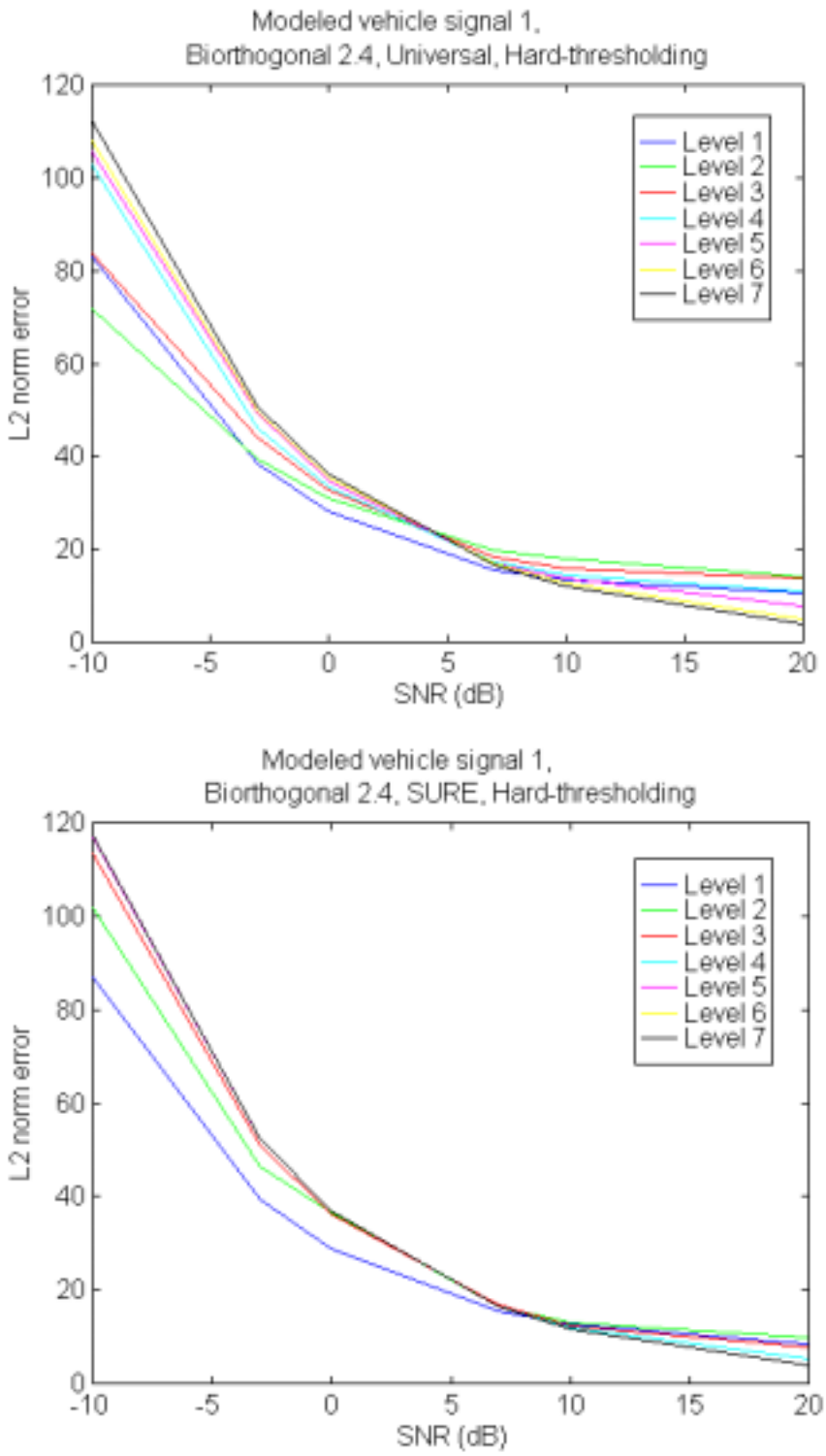

Figure 2.20 L_2 Norm Error of Different Decomposition-Reconstruction Level using Wavelet Basis Biorthogonal 2.4, (1) Universal, (2) SURE Threshold is Applied

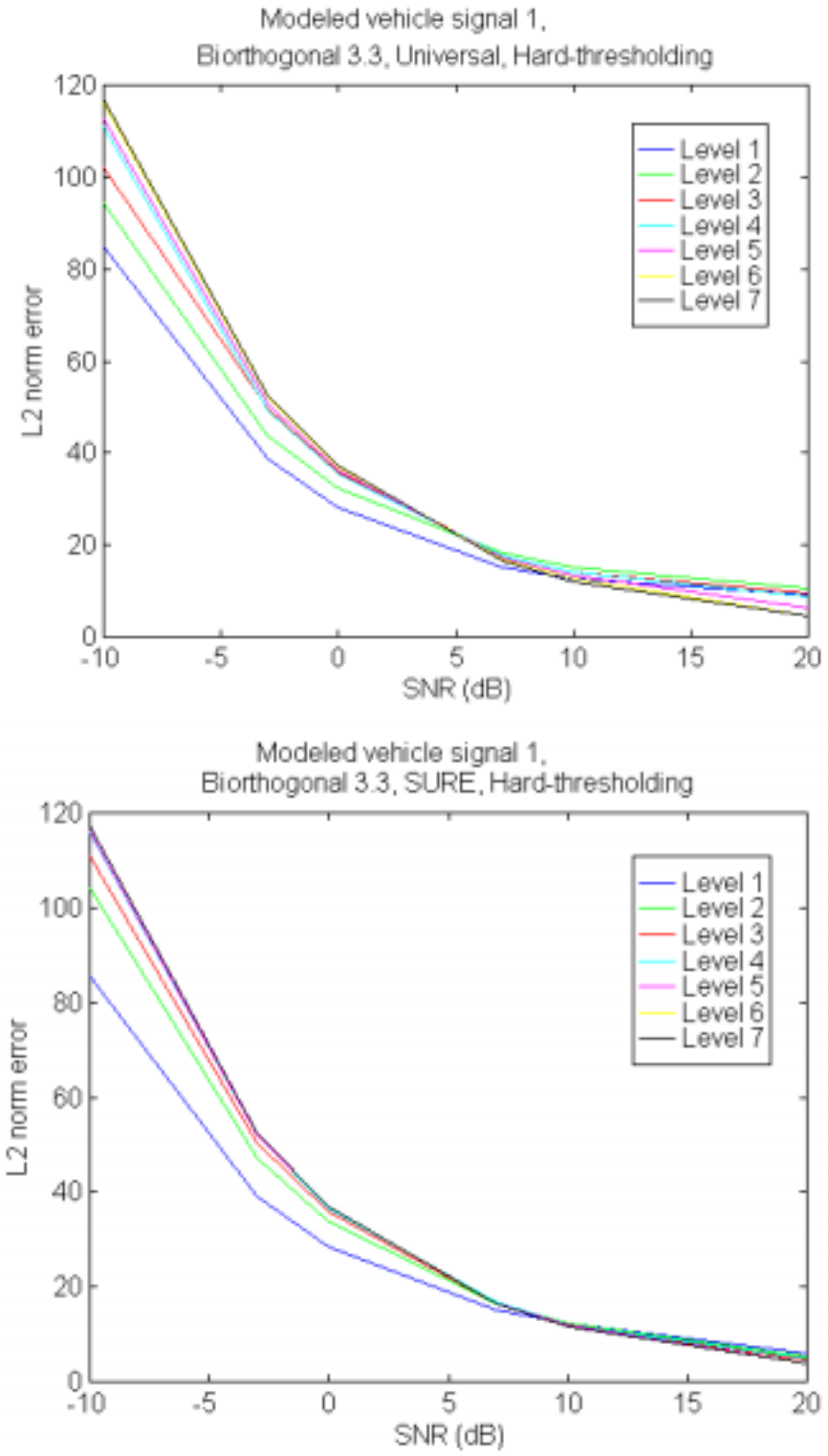

Figure 2.21 L_2 Norm Error of Different Decomposition-Reconstruction Level using Wavelet Basis Biorthogonal 3.3, (1) Universal, (2) SURE Threshold is Applied

larger the level the less error incurred; and in the lower SNR region, the larger the level the more error incurred. This is true for both the Universal and SURE thresholds.

One may notice that in the test of L_2 norm sensitivity of different decomposition-reconstruction levels, the level-1 performs relatively well. However this may be due to a bias in the vehicle data being used.

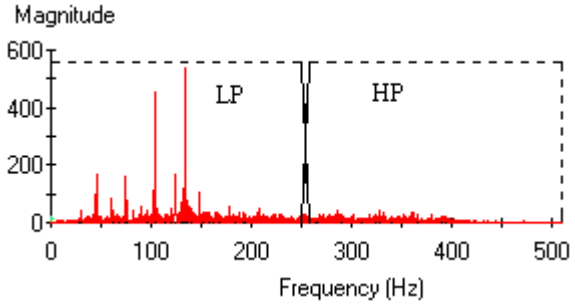

Figure 2.22 Frequency Response of Modeled Vehicle Signal

The frequency response of the modeled vehicle signal is shown in Figure 2.22. Clearly, if the signal is decomposed by a level 1 PWT, most of the energy will be concentrated in the lower frequency band. In the de-noising algorithm, the coefficients residing in the lowest frequency band are not subject to thresholding. Therefore, after de-noising, the coefficients in the lowest frequency band remain the same since these coefficients are "viewed" to contain most of the signal energy. Now in the event the majority of the signal energy resides within the lowest frequency band of the first partition of a level one decomposition, this leads to the "artifact" that the level-1 decomposition results in a good level choice for de-noising.

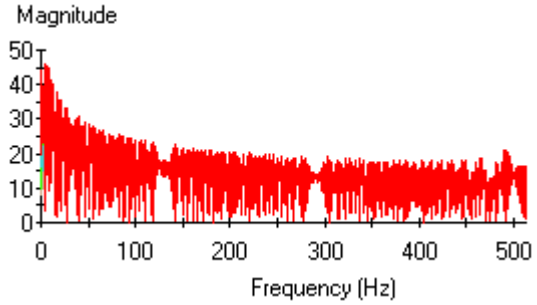

Figure 2.23 Frequency Response of the Chirp Signal.

In order to perform a more even-handed study of the sensitivity of de-noising to decomposition level choices the Chirp signal is used as another test input signal. The frequency response of the Chirp signal is shown in Figure 2.23. It spreads out across the entire frequency band of interest. Since the L_2 norm error plots are similar to the plots using the modeled vehicle signal as the input, Table 2.7 is used to briefly summarized the pertinent results obtained using the Chirp signal and the trends observed. From the Chirp signal test, some conclusions can be drawn with respect to the empirical data summaries presented in Table 2.7 concerning the sensitivity of the de-noising process to the selection of decomposition level.

1. In Daubechies and Coiflet studies, middle range levels on the order of level-3, level-4, or level-5 tend to perform better than the rest of the levels.
2. In Biorthogonal study for lower SNR range, the larger the level the more error incurred. Also, after a large enough level selection, for example, level-5 or 6, the error seems to reach a steady state and does not appear to grow substantially. If the SURE threshold is applied, since there is no obvious crossover point, level 1 wins all. If Universal is applied, the best performer tends to increase to level 3 when the SNR increases.

Table 2.7 Comments for L_2 Norm Errors in Different SNR Ranges. L_i stands for level-*i* Decomposition-Reconstruction. T_U stands for Universal threshold, T_S stands for SURE Threshold.

Basis function	Daubechies			
Support	6		12	
Threshold	T_U	T_S	T_U	T_S
-10 ~ 0 dB	Error spreads from 25~70. L_5 performs best.	L_4 and L_5 perform better than others do.	Error spreads from 30~95. L_4 performs best.	Error of L_5 ~L_7 stick together. L_4 performs best.
0 ~ 10 dB	L_5 ~ L_7 perform better than others do.	L_5 performs best.	Error of $L_4 < L_5$,$L_3 < L_2$, $L_6 < L_1$, L_7	Error of L_5 ~L_7 stick together. L_4 performs best.
10 ~20 dB	Error within 5. L_3 ~L_7 perform the same well.	Error spreads< 5. L_5 performs best.	Error spreads< 5. L_5 performs best.	Error spreads< 5. L_4 performs best.

Basis function	Coiflet			
Support	18		30	
Threshold	T_U	T_S	T_U	T_S
-10 ~ 0 dB	Error spreads from 30~100. L_4 performs best.	L_4 performs best.	Error of L_6 ~L_7 stick together. L_4 performs best.	Error of L_4 ~L_7 stick together. L_3, L_1 perform better.
0 ~ 10 dB	L_5 performs best.	L_4 performs best.	Error of L_6 ~L_7 stick together. L_4 performs best.	All levels stick together. L_2, L_3 perform better.
10 ~20 dB	Error spreads< 5. L_5 performs best.	All levels stick together. L_4 performs best.	Error of L_5 ~L_7 stick together. L_4 performs best.	All levels stick together. L_2 performs best.

Basis function	Biorthogonal			
Support	Bior2.4: highpass=3, lowpass=9		Bior3.3: highpass=4, lowpass=8	
Threshold	T_U	T_S	T_U	T_S
-10 ~ 0 dB	L_2 and L_3 perform better than others do.	L_1 performs best.	Error spreads from 75~100. L_1 performs best.	L_1 performs best.
0 ~ 10 dB	L_3 performs best.	All levels stick together. L_1 performs best.	Error spreads< 5. L_2, L_3 perform better.	All levels stick together. L_1 performs best.
10 ~20 dB	Error spreads< 5. L_3 performs best.	All levels stick together.	Except L_1 performs worst, others stick together.	All levels stick together.

3. CONCLUSIONS

The results of our initial investigation of the potential for the Packet Wavelet Transform (PWT) de-noising as a vehicle signal pre-processor has proved very promising. A significant amount of machinery was built to support this investigation. The initial set of software is now fully integrated with the VSAE. We have an initial set of benchmarks via a set of sensitivity studies on the effectiveness of various parameters settings afforded by the PWT de-noising method. These benchmarks/studies will provide guidance in selecting the more capable configurations for a PWT-based vehicle signal pre-processor.

From these initial set of sensitivity studies, no overall set of parameters walk away with the ultimate optimization set point for the vehicle signal problem. This is to be expected, however by examining the results of the individual sensitivity studies over the following variables individually tested: 1) threshold application method (e.g.. hard verses soft), 2) threshold values (e.g. Universal, Minimax, SURE, Hybrid), 3) different wavelet basis functions (Daubechies, Coiflet, Symlets, Beylkin, Biorthogonal, etc.), 4) filter support (i.e. length of the basis wavelet filters), and 4) decomposition-reconstruction level (i.e. length of Packet Wavelet Full Tree) and by choosing to optimize over a given sub-range of the SNR sensitivities conducted one can certainly reduce the number of viable choices to a manageable few for further testing and configuration as a vehicle signal pre-processor.

An important consideration for the application of this pre-processing method is the reduction to a real-time vehicle monitor application. We are currently considering the role of various windowing schemes coupled with the PWT de-noising operation to segment this operation over very long time horizons which will allow recovering in a sub-optimal fashion as much of the benefit of the de-noising operation that is accrued when operating on the entire vehicle signal support.

4. ACKNOWLEDGEMENTS

This work was supported under the SBIR program of the U.S. ARMY ARDEC/TACOM, Picatinny Arsenal, NJ 07906-5000 under contract number DAAE30-98-C-1067.

5. REFERENCES

1. Barsanti, Jr. R. J., "*De-noising of Ocean Acoustic Signals using Wavelet-based Techniques.*" Master's thesis, Naval Postgraduate School, Monterey CA, Dec. 1996.
2. Daubechies, I., *Ten Lectures on Wavelets*, SIAM, Philadelphia PA, 1992.
3. Strang, G., and Nguyen, T., *Wavelets and Filter Banks*, Wellesley-Cambridge Press, 1996.
4. Vaidyanathan, P. P., *Multirate Systems and Filter Banks*, Prentice-Hall, Inc., 1993.
5. Lo, J., *"Fault Prediction and Classification for Condition-Based Maintenance using Wavelets."* Master's thesis, Pennsylvania State University, May 1998.
6. Vetterli, M., and Kovacevic, J., *Wavelets and Subband Coding*, Prentice-Hall, Inc., 1995.
7. Johnstone, L. M., and Silverman, B. W., *"Wavelet Threshold Estimators for Data with Correlated Noise."* Aug. 1996.
8. Donoho, D., and Johnstone, I., *"Adapting to Unknown Smoothness via Wavelet Shrinkage"*, Dept. of Statistics, Stanford University, July 1994.
9. Stein, C., "*Estimation of the Mean of a Multivariate Normal Distribution," The Annals of Statistics*, Vol. 9, pp. 1135-1151, 1981.
10. Donoho, D., and Johnstone, I., *"Minimax Estimation via Wavelet Shrinkage"*, Dept. of Statistics, Stanford University.
11. Kalker, A. A. C., and Shah, I. A., *"Ladder Structures for Multidimensional Linear Phase Perfect Reconstruction Filter Banks and Wavelets."* SPIE Visual Communications and Image Processing 92, vol. 1818, pp. 12-20.
12. Vaidyanathan, P. P., and Hoang, P. Q., *"Lattice Structures for Optimal Design of Two-Channel Perfect-Reconstruction QMF Banks,"* IEEE Trans. ASSP 36, 1988.
13. Krauss, T.P., Shure, L., and Little, J.N., *Signal Processing Toolbox User's Guide*, The Mathworks, Inc. Feb. 1994.